JSAEM Studies in Applied Electromagnetics and Mechanics, 11

APPLICATIONS OF ELECTROMAGNETIC PHENOMENA IN ELECTRICAL AND MECHANICAL SYSTEMS

Proceedings of
The First Japanese-Australian Joint Seminar on Applications of Electromagnetic Phenomena in Electrical and Mechanical Systems
16-17 March 2000, Adelaide, Australia

Editors:

Andrew Nafalski **Mahmoud Saghafifar**
University of South Australia, Adelaide, Australia

Applications of Electromagnetic Phenomena in Electrical and Mechanical Systems
A. Nafalski and M. Saghafifar (eds)

The eigen pattern of graphics and its application to the magnetic field identification

Kenichi Wakabayashi, Seiji Hayano, and Yoshifuru Saito
Graduate School of Engineering, Hosei University

Tosiyasu L. Kunii
Computational Science Research Center, Hosei University

Kiyoshi Horii
Shirayuri Women's College

ABSTRACT: A new concept is introduced to extract the essential and distinct characteristics of the magnetic field distributions. A key idea is to introduce the eigen patterns, which represents the characteristics of magnetic fields independent of their resolutions and space coordinates. We apply the notion of eigen patterns to magnetic fields identification of the electric circuit element. As a result, we have succeeded in identifying the tested magnetic field distributions.

1 INTRODUCTION

Modern electronic and electrical engineering take electromagnetic field distributions into account for the design of electric and electronic devices operating at high frequencies [1-2]. For example, cellar-phones and personal computers are composed of a large number of semiconductor elements and of the electric circuits with extremely high density.

For such high-density electronic circuits, The former is simple and reliable but it is essentially required to measure the magnetic fields with great preciseness. The latter is a further difficult approach because it requires solving an inverse problem [3-4].

In the present paper, we propose a new concept extracting the essential and distinct characteristics of the magnetic field distribution around electronic devices. This new concept is based on an eigen pattern, which represents the characteristics of magnetic field distribution independent of the resolutions and space coordinates.

inspection as well as testing lead to a serious difficulty. To break through this difficulty, one of the most reasonable methods is to employ a nondestructive method utilizing a magnetic field essentially accompanying with the operation of electronic devices.

Nondestructive testing utilizing magnetic fields can be classified into two major categories: one is the pattern recognition of magnetic field distributions, and the other is to evaluate the current distributions in electronic devices. The eigen pattern of a magnetic field distribution is obtained by projecting the three orthogonal magnetic field vector components onto the x-, y- and z- coordinate system. Thereby, this projection takes the space coordinate information, and extracts the essential vector characteristics of the target magnetic field distribution.

We apply this method to the magnetic field visualization and to the pattern recognition for the nondestructive inspection of the electronic devices. Intensive simulation suggests that our eigen pattern method is one of the powerful methodologies for the nondestructive testing of electronic devices.

2 EIGEN PATTERN OF GRAPHICS IMAGE

Key idea

A color graphics image on a x-y plane coordinate system is represented by a set of pixels containing the red, green and blue color information:

$$\begin{aligned} &image \in pixel_{i,j}, \\ &pixel_{i,j} \in f_r(x_i, y_j), f_g(x_i, y_j), f_b(x_i, y_j), \\ &i = 1,2,..,m, \quad j = 1,2,..,n, \end{aligned} \tag{1}$$

Where *m and n* are the entire number of pixels in the direction of *x and y* axes. The subscripts *r, g and b* refer to the red, green and blue colors, respectively. Also, the functions in Eq. (1) take the values between 0 and 1

$$\begin{aligned} &0 \le f_r(x_i, y_j) \le 1, \\ &0 \le f_g(x_i, y_j) \le 1, \\ &0 \le f_b(x_i, y_j) \le 1, \\ &i = 1,2,..,m, \quad j = 1,2,..,n. \end{aligned} \tag{2}$$

Let us consider a red-green-blue (RGB in short) orthogonal coordinate system, denoting the resolutions of the red, green and blue axes by *R, G and B*. Then a set of functions $g(r_o, g_p, b_q)$, represent the image as

$$\begin{aligned} &image \in g(r_o, g_p, b_q), \\ &r_o \in f_r(x_i, y_j), \\ &g_p \in f_g(x_i, y_j), \\ &b_q \in f_b(x_i, y_j), \\ &o = 1,2,..,R, \quad p = 1,2,..,G, \quad q = 1,2,..,B, \\ &i = 1,2,..,m, \quad j = 1,2,..n. \end{aligned} \tag{3}$$

A normalized value of the function $|g(r_o, g_p, b_q)|$ in Eq. (3) takes a value between 0 and 1

$$\begin{aligned} &0 \le \left| g(r_o, g_p, b_q) \right| \le 1, \\ &o = 1,2,..,R, \quad p = 1,2,..,G, \quad q = 1,2,..,B. \end{aligned} \tag{4}$$

The functions in Eq. (3) are given by

$$\begin{aligned} &\textit{Initial} \quad \text{condition:} \quad g(r_o, g_p, b_q) = 0, \\ &\text{If} \quad r_o = f_r(x_i, y_j), g_p = f_r(x_i, y_j), b_q = f_r(x_i, y_j), \\ &\text{then} \quad g(r_o, g_p, b_q) = g(r_o, g_p, b_q) + 1, \\ &o = 1,2,..,R, \quad p = 1,2,..,G, \quad q = 1,2,..,B, \\ &i = 1,2,..,m \quad j = 1,2,..,n, \\ &\textit{Final} \quad \text{normalizaton} \quad \frac{g(r_o, g_p, b_q)}{Max \left[g(r_o, g_p, b_q) \right]} \end{aligned} \tag{5}$$

Uniqueness of eigen pattern

Considering an image having 1 by 1 pixel, then

$$\begin{aligned} &r_1 = f_r(1,1), \quad 0 < r_1 \le R, \\ &g_1 = f_g(1,1), \quad 0 < g_1 \le G, \\ &b_1 = f_r(1,1), \quad 0 < b_1 \le B \end{aligned} \tag{6}$$

are uniquely determined with the resolutions *R* in red axis, *G* in green axis and *B* in blue axis, so that the function $g(r_1, g_1, b_1)$ becomes

$$g(r_1, g_1, b_1) = 1, \tag{7}$$

Where the dynamic range of *R, G and B* in Eq.(6) depend on the original color resolutions, e.g., 24-bits bitmap form. It is obvious that each of the images with a large number of pixels has its distinct eigen pattern. Conversely, each of the eigen patterns identifies a distinct image within the given original resolution.

Visualization of the magnetic field

In order to apply the eigen patterns to the magnetic fields, we visualize them by regarding the x-, y- and z-magnetic field components as red, green and blue color components, respectively. Here, each of the components is normalized to satisfy the Eq.(2). Fig.1 shows the x-,y- and z-magnetic field components and the RGB color visualized magnetic field distribution. The position of pixel corresponds to the measurement point. Thus we can extract the eigen patterns from the RGB visualized magnetic fields

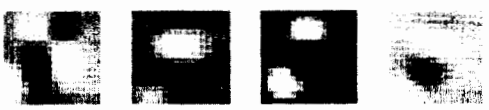

(a) (b) (c) (d)

Figure 1 Magnetic field components and color image.
(a) x-component, (b) y-component,
(c) z-component, and (d) visualized magnetic field.

3 GRAPHICS IMAGE SYSTEM OF EQUATIONS

3.1 Input vector

Consider a test eigen pattern with R by B by G resolution:

$$E_T \in g_T(i,j,k) \quad i=1,2,..,R, \quad j=1,2,..,G, \quad k=1,2,..,B, \tag{8}$$

Arranging the numerical values of pattern E_T into a column-wise form gives an input vector $\mathbf{Y}$ with $R\times G\times B$-th order as:

$$\mathbf{Y}=[g_T(1,1,1), g_T(2,1,1),.., g_T(R,1,1), g_T(1,2,1), g_T(1,3,1),.., g_T(1,G,1), g_T(1,1,2), g_T(1,1,B),.., g_T(R,G,B-1), g_T(R,G,B)]^T. \tag{9}$$

3.2 System matrix

Assume the $p-th$ database eigen patterns with R by B by G resolution

$$C_D^{(n)} \in g_D^{(n)}(i,j,k) \quad i=1,2,..,R, \quad j=1,2,..,G, \quad k=1,2,..,B, \quad l=1,2,..,p. \tag{10}$$

Similar to Eq.(9), $l-th$ vector of the system matrix ($\mathbf{d}^{(l)}$) is given by:

$$\mathbf{d}^{(l)}=[g_D^{(l)}(1,1,1), g_D^{(l)}(2,1,1),.., g_D^{(l)}(R,1,1), g_D^{(l)}(1,2,1), g_D^{(l)}(1,3,1),.., g_D^{(l)}(1,G,1), g_D^{(l)}(1,1,2), g_D^{(l)}(1,1,B),.., g_D^{(l)}(R,G,B-1), g_D^{(l)}(R,G,B)]^T. \tag{11}$$

Thus, a system matrix with $R\times G\times B$ -th rows and p-th columns is represented by

$$D=[\mathbf{d}^{(1)}, \mathbf{d}^{(2)},.., \mathbf{d}^{(p)}] \tag{12}$$

3.3 System of equations

Denoting a solution vector $\mathbf{X}$ with order p, a system of graphics image equations is formally written by

$$\mathbf{Y}=D\mathbf{X}. \tag{13}$$

In most case, the number of equations $R\times G\times B$ is much greater than that of the unknowns in vector x with order p; Therefore, it is possible to apply a conventional least square means as in [5]:

$$\mathbf{X}=[D^T D]^{-1} D^T \mathbf{Y}. \tag{14}$$

3.4 Image visualization and identification

By considering the input vector $\mathbf{Y}$ in Eq.(9) and the column vector $\mathbf{d}^{(k)}$ in Eq.(11), it is revealed that the elements in the solution vector $\mathbf{X}$ are the weights $w_i (i=1,2,..,p)$ of the database images.

This means a visualized image $V_{m\times n}$ is composed of:

$$V_{m\times n}=\sum_{i=1}^{p} w_i C_{m\times n}^{(i)}. \tag{15}$$

When $w_1=1$ and the other weights are zero in Eq.(15), then the image is the same as the first database image. In other words, the test image is identified as the first database image.

4 EXAMPLE

The problem is to identify the shapes of coils by means of least squares along with the eigen patterns.

The fundamental difference between the RGB color computer graphics and the vector fields is that the red, green and blue components in computer graphics are always fixed to an absolute coordinate system, whereas the physical vector fields are always measured in a relative orthogonal coordinate system. In order to overcome this difficulty, we have to decide on a reference coordinate system.

The system can be in 4 directions (plus and minus-x, plus and minus-y). The sum of the direction x components takes the maximum facing the positive direction of the x-axis. Similarly, the direction y-components takes the maximum facing the positive direction of the y-axis. Here, z-axis is fixed.

Fig.2(a) shows the 4 magnetic field distributions of the same element measured on the distinct coordinate systems. Fig.2(b) shows the magnetic field distribution on the reference coordinate system.

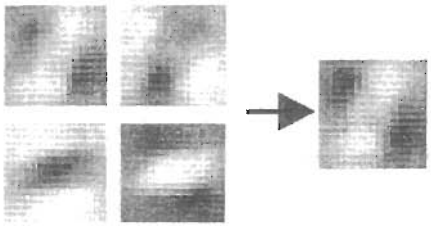

(a) (b)

Figure 2 Reference coordinate system.
(a) Magnetic field distribution measured on the distinct coordinate systems
(b) On the reference coordinate system

4.1 Input images

We have measured the magnetic field distributions for the tested coils. Figs.3(a)-(c) show the visualized magnetic field images (upper) and tested coils (lower) when the output voltage of the sensor coil located at each measurement point takes a maximum in value. Each of the orthogonal magnetic field components is measured by changing the direction of the solenoidal sensor coil. The number of measurement points is 15×15. Fig.3(d) shows the compound model containing the elements in Figs. 3(a)-(c) with the number of measurement points, 16×16.

4.2 Database images

Fig.4(a) shows the compound model. Fig.4(b) shows 25 database images with 7×7 pixels cut out from the compound model with moving 2 pixels to lengthwise and crosswise. To satisfy the condition in (2), the maximum values representing the images in Fig.4(b) are normalized to 1.

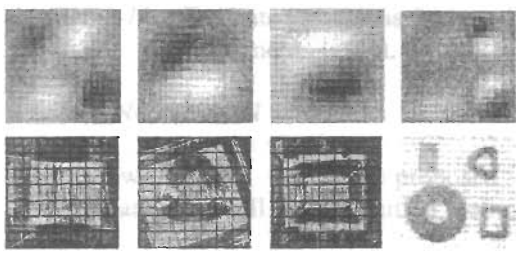

(a) (b) (c) (d)

Figure 3 RGB visualized images (upper) and coil elements (lower).
(a) Twisted around a board, (b) Triangle,
(c) Rectangle, (d) Compound model

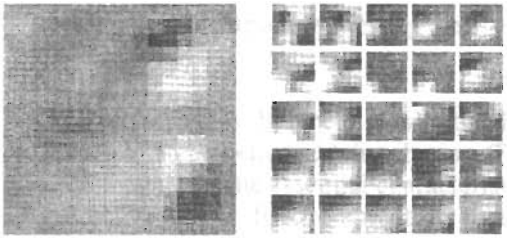

(a) (b)

Figure 4 RGB visualized images.
(a) Compound model
(b) Database images

4.3 Solution

After evaluating a simple least square solution using Eq. (14), the visualized images by Eq. (15) are shown in Fig.5 (the upper side). The lower side of Fig.5 shows the identified images in the database. In order to examine the validity of the recovered images, Fig.6 shows the elements of the solution vectors.

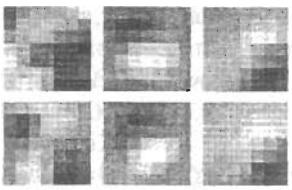

(a) (b) (c)

Figure 5 Recovered (upper) and identified (lower) images.
(a) Twisted around a board
(b) Triangle
(c) Rectangle

In Figs.6(b)-(c), especially (c), the position 25 corresponds to the correct image demonstrating our strategy yields good results. But Fig.6(a) contains some noises, reducing the quality of the recovered image in Fig.5(a). In the case of a complicated magnetic field distribution that has some ups and downs like Fig.3(a), measurement errors tend to increase them when the number of measurement points decreases. We can obtain better solutions by measuring the magnetic field distributions in detail. Fig.7(a) shows the estimated positions of the distinct elements in the compound model obtained by taking an element having the maximum value from each of the solution vectors. Fig.7(b) shows the tested layout of the elements. Thus, we have succeeded in estimating the correct layout.

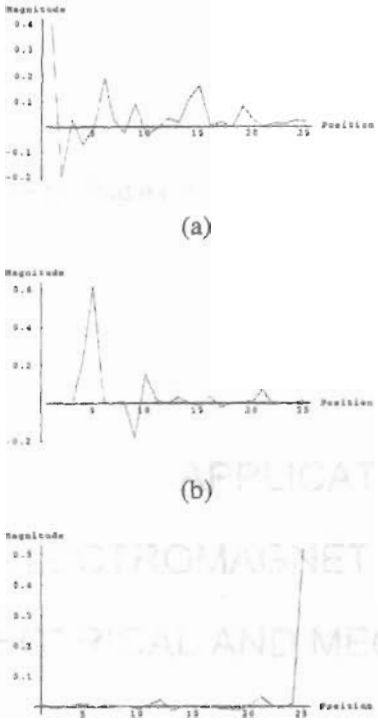

(a)

(b)

(c)

Figure 6 Elements of the solution vector.
(a) Twisted around a board
(b) Triangle
(c) Rectangle

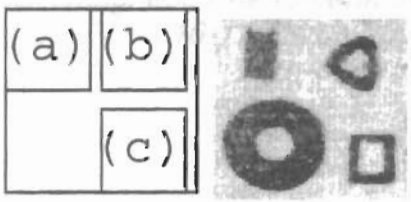

(a) (b)

Figure 7 (a) Estimated positions (b) tested coil elements layout.

5 CONCLUSION

As shown above, we have proposed a new visualization as well as recognition methodology for the nondestructive testing of electronic devices [6].

Our methodology has been based on the eigen pattern of a magnetic field distribution. The eigen pattern contains the essential characteristic of the distinct magnetic field distribution independent of the magnetic field measuring space coordinate systems. In the present paper, we have succeeded in recognizing the distinct element as well as estimating the distinct position from the compound model. Thus, the magnetic field visualization using eigen patterns is one of the most powerful and effective nondestructive strategies for inspecting electronic devices.

6 REFERENCES

1 Hayano, S., Saotome, H., Nakajima, Y., and Saito,Y., A new type of high frequency transformer, *IEEE Transaction on Magnetics*,Vol.MAG-27, No.6, Nov., (1991), pp. 5205-5207.

2 Midorikawa,Y., Hayano, S. and Saito, Y., A new inductor having a noise filtering capability, *IEEE Transaction on Magnetics*, Vol.MAG-30, No.6, Nov., (1994), pp.4761-4763.

3 Yoda, K. and Saito, Y., A wavelet transform approach to inverse problem of Vandermonde type systems, *IEEE Transaction on Magnetics*, Vol.MAG-33, No.2, March, 1997, pp.1955-1957.

4 Yoda, K., Saito, Y. and Sakamoto, H., Dose optimization of proton and heavy ion therapy using generalized sampled pattern matching, *Phys.Med.Biol.* IOP Publishing, 1997, pp.2411-2420.

5 Strang, G., *Linear Algebra and its Applications*, 1976, Academic Press, Inc.

6 Wakabayashi, K., Hayano, S. and Saito, Y., Eigen Pattern of the Magnetic Field and its Application to the Nondestructive inspections, *Digest of the Joint Seminar*, November, 1999.